Heave Motion Estimation on a Craft Using a Strapdown Inertial Measurement Unit

Øyvind F. Auestad [*,**] **Jan T. Gravdahl** [*] **Thor I. Fossen** [*]

[*] *Dept. of Eng. Cybernetics, NTNU, N-7491 Trondheim, Norway;*
e-mail: oyvind.auestad@itk.ntnu.no
[**] *Umoe Mandal AS, N-4515 Mandal, Norway*

Abstract: This paper deals with heave position and heave velocity estimation on a craft. The estimation is done without any knowledge of the specified craft. An accurate estimation of these signals is useful when one wants to control or monitor the heave motions on a platform or a ship such as in a active heave compensated systems. The necessary sensor input for the proposed guidance system is a strapdown inertial measurement unit (IMU) which consists of three gyroscopes and three accelerometers. In this case study, the heave motion estimation is required as input for a control system on a Surface Effect Ship (SES) where it is desired to control the air cushion pressure in order to damp vertical motions. The motions are induced by sea wave propagations. A SES will experience high frequency accelerations on the hull compared to other vessels. A lift fan sets up these accelerations or process disturbances and complicates the performance of the estimation. The estimation is performed using an observer. The observer model is based on a set of superimposed sinusoidals, each with a different excitation frequency. The sum of these denotes the actual heave motion. The estimation algorithm is adaptive in terms of changes in the sea states. Results will be given using real experimental data from model tests of a 3 meter long SES.

Keywords: Observer, strapdown systems, Inertial measurement units, Spectral analysis

1. INTRODUCTION

Several methods for estimating heave motion is available both in literature and on the market. One approach is to aid the IMU with external sensors such as lasers, acoustic or GPS measurements. The latter is done in Fossen and Perez [2009]. However, external aiding usually results in higher costs and dependency on the external sensor. In this paper, only systems with a low cost such as a strapdown Micro-Electro-Mechanical Sensor (MEMS) IMU as sensor measurement are considered.

MRU H [Kongsberg, 2013] is an example of what is available on the market. The Motion Reference Unit (MRU) offers high accuracy but suffers from a high purchasing cost. Godhavn [1998] presents the Seatex MRU which accurately estimates the heave motion using an adaptive heave filter algorithm. The filter minimizes measured acceleration error sources such as bias and noise by adaptively changing the cut off frequencies of a bandpass filter. Kongsberg now owns Seatex.

The approach used in this paper is based on Küchler et al. [2011]. Küchler estimates heave motion using a single accelerometer and shows results both in simulation and through a test bed that consist of two winches and a hook. This paper estimates the motion in a similar way but transfers the motion to a different point on the vessel. Results will be given using real experimental data of a 3 meter long SES with severe process disturbance. Also, the implemented proposed observer has been altered from an EKF to a linear discrete time Kalman Filter without any loss of generality or functionality. The proposed system is Linear-Time-Invariant (LTI) which ensure that the Kalman Filter will converge towards a steady-state.

1.1 Motivation

The case studied in this paper involves the Umoe Mandal's Offshore Service Vessel named The Wave Craft. The Craft is designed for service missions to offshore wind-turbines. The craft is a SES, which rides on an air cushion enclosed by catamaran twin hulls and flexible rubber seals in the bow and in the stern. The air cushion is pressurized using centrifugal lift fans that lifts the vessel towards the water surface leaving only a small portion of the side hulls in the water. The cushion pressure can be altered by controlling the air cushion outflow leakage area. Altering the opening angle of an installed ventilation valve does this. It is damping of the bow tip that is of interest since this is the area where the service personnel will leave the vessel and board the turbine. Is is therefore important that the motion estimation occurs at this point.

Due to the cushion dynamics, the strapdown accelerometers will experience severe process disturbances. These disturbances are unwanted on the estimated heave motion. The magnitudes of these accelerations are varying along the longitudinal position of the ship. Therefore, the model test setup was set up using two options that possibly would alter the performance of the estimation. At the first approach, the IMU, with the accelerometers, was placed amidships where the magnitude is assumed low. The motion was transferred to the bow tip using a coordinate

transformation. The second approach, which is denoted the direct approach, consist of placing the IMU directly at the vessel bow tip.

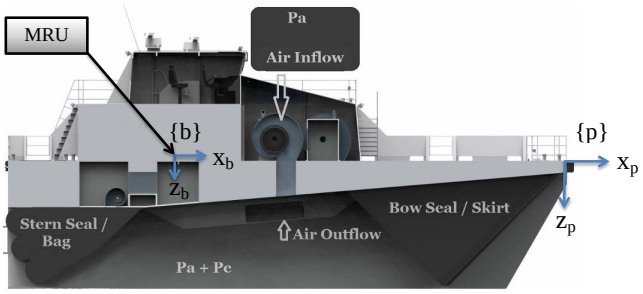

Fig. 1. The SES Concept (Umoe Mandal (UM) Proprietary). Two coordinate systems are defined. The $\{b\}$ frame is body fixed with its origin located at the IMU. Denote the linear translation along the z_b axis as z. The $\{p\}$ frame is formulated with the z_p axis pointing downwards normal to the Earth's surface. The origin is located at the vessel bow tip. Denote the translation along this axis as D. Motion in z and D are both referred to as heave. Both coordinate systems use the right hand rule to determine rotation signs.

Auestad et al. [2013] presents a SES simulator and a control system for damping vertical motions at the bow. This is done by altering the cushion pressure using feedback from the heave motion at the craft's nose tip. An actuator that controls the opening of the ventilation valve will act proportionally to the heave motion. This will arrange for safer transfer of personnel and goods from vessel to turbine foundation. The craft is assumed free floating at zero craft speed. The article assumes that the heave motion is known. In reality, heave velocity is simple to obtain, while heave position is not. Accelerometer measurements are affected by noise and bias. The errors accumulate by the number of times this signal is integrated. Hence, estimating heave position is harder than estimating heave velocity.

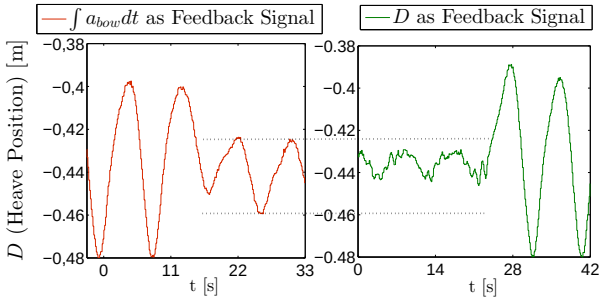

Fig. 2. The plot shows the effect of a long crested regular wave, $T_p = 8.5$s. D is measured by lab equipment and $\int a_{bow}\, dt$ was given by numerical integration of a high-pass filtered accelerometer signal. The accelerometer was attached at the origin of the $\{p\}$ frame.

Figure 2 shows time series for the heave position (expressed in {p}) from a model test where the vertical wave induced motions are being damped. The control system is inactive at the beginning and at the end of the left and right sub-figure respectively. This corresponds to a constant air cushion pressure. The control system is active for the remaining part and note that the amplitude of the right sub-figure is smaller than of the left. Hence, when the craft faces a long crested wave, such as in this case, the performance is increased when D (see fig. 1) is available. The wave period as denoted T_p.

2. HEAVE MOTION ESTIMATION

The task of this paper is to estimate $\dot{D}$ and D using an IMU as illustrated in figure 1. Define: $\hat{\mathbf{D}} := \left[\hat{\dot{D}}, \hat{D}\right]^T$ and $\hat{\mathbf{z}} := \left[\hat{\dot{z}}, \hat{z}\right]^T$. $\hat{\mathbf{D}}$ is the output of the estimator.

The proposed method for estimating heave motion involves four steps that will be explained in the following. The first three steps are based on [Küchler et al., 2011] while the latter one consist of transforming the motion from the {b} to the {p} frame.

The input for the estimator and the necessary signals from the IMU, is roll rate, pitch rate and linear acceleration along the z_b axis. Denote these as p_{imu}, q_{imu} and $a_{z,imu}$, respectively.

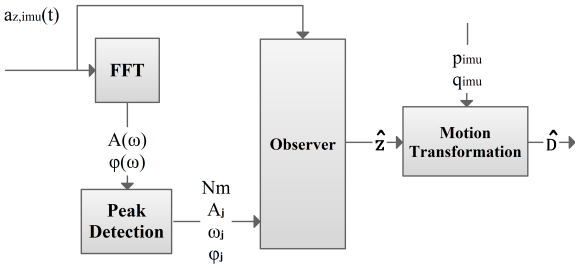

Fig. 3. Illustration of the four necessary steps in order to estimate heave motion.

The estimator model is based on including all forms of waves that will excite craft motions. Heave position, $z = z(t)$, can be modelled as a set of N_m overlaying sine waves [Chakrabarti, 2008]:

$$\begin{aligned} z(t) &= \sum_{j=1}^{Nm} A_j cos(\omega_j t + \varphi_j) + v(t) \\ &:= \sum_{j=1}^{Nm} z_j(t) + v(t) \overset{v=0}{=} \sum_{j=1}^{Nm} z_j(t) \end{aligned} \tag{1}$$

where $j = 1, 2, .., Nm$, A_j, ω_j and φ denotes amplitude, eigenfrequency and phase of each sine wave. Each wave is denoted as a mode. $v(t)$ is included to capture slowly varying effects such as the tidal range. Since our problem only concerns relative heave motion, $v(t)$ is neglected for the rest of the analysis.

2.1 Step 1 - Fast Fourier Transform (FFT)

Eq. (1) is described in the time domain. It can be expressed in the frequency domain using a wave energy spectrum [Faltinsen, 1993]. The spectrum is calculated online using a FFT with a chosen memory length that is sufficiently small to ensure smooth spectral curves. Let $\ddot{A}(\omega)$ and $\ddot{\varphi}(\omega)$ denote the amplitude and phase spectrum of the acceleration signal (therefore the double dot). The wave spectrum

illustrates the energy that acts in heave acceleration as a function of frequency.

Figure 3 and eq. (1) indicates that it is the spectrum of heave position that are of interest, and not the heave acceleration spectrum. However, a spectrum transformation from acceleration to position can be calculated directly using:

$$A(\omega) = \frac{\ddot{A}(\omega)}{\omega^2}, \quad \varphi(\omega) = \ddot{\varphi}(\omega) - \pi, \quad \omega > 0 \tag{2}$$

The accuracy of the estimation is dependent on chosen sampling time of the FFT which gives the spectrum a desired resolution in the frequency plane. In the next section we will see that this corresponds to the number of modes (N_m) that will appear. The window length of the FFT must include and detect the highest frequency of the sea state as well as potential, relevant eigenfrequencies of the craft that might be excited.

2.2 Step 2 - Peak Detection

Figure 4 illustrates the amplitude spectrum discussed in section 2.1. The peak detection consist of localizing every local maximum of $|A(\omega)|$. Every maximum corresponds to a mode j, where $j = 1, 2, ..., N_m$.

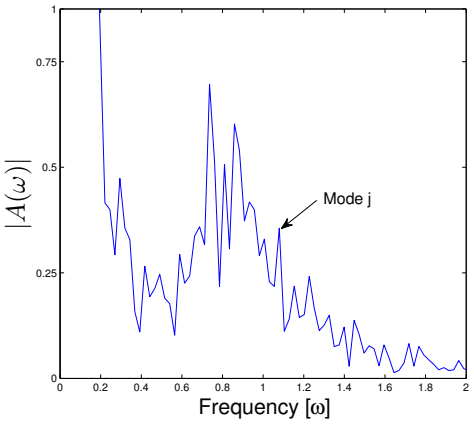

Fig. 4. The normalized amplitude of the frequency response. As the figure indicates, this specific wave has a period of 8.5 seconds ($\omega \approx 0.8$) where the majority of the energy is stored. The tests were performed in a wave tank [1]

Each mode has a specific amplitude (A_j), phase (φ_j) and eigenfrequency (ω_j). This is the output of the peak detection algorithm. In order to avoid singularities, modes with eigenfrequency equal to zero or modes that are sufficiently close to a neighbour mode must be removed. In order to handle changes in the sea states, the peak detection must be repeated every fixed time interval T.

[1] All figures containing time series/frequency response, are from model tests of the Wave Craft, performed in cooperation between, SINTEF/Marintek, Umoe Mandal and NTNU. Test results in this paper were performed both at the *MC Lab, NTNU*, and the *Ship Model Tank, Marintek*.

2.3 Step 3 - Observer

An observer is required since the FFT only considers mean values over a finite time horizon. By setting $v = 0$ in eq. (1), each mode is considered a solution to an undamped oscillator The following ordinary differential equation describes the dynamics of the oscillator:

$$\ddot{z}_j + \omega_j^2 z_j = 0, \quad t > t_0, \tag{3}$$

where $j = 1, 2, ..., N_m$. The initial conditions of (3), namely $z_j(t_0)$ and $\dot{z}_j(t_0)$ are given according to (1) and by differentiating (1) along its system trajectories using the output from the peak detection algorithm, t_0 denote the time whenever the system needs to be re-initialized. In order to keep the decay time down, one must only re-initialize the system whenever a new mode j is either detected or vanished from the output of the peak detection algorithm. This mode, is respectively, added or removed from the system. The system needs to be adaptive in terms of changes in the sea state, therefore, the dynamics of the eigenfrequencies, ω_j, are modeled as random walk parameters:

$$\dot{\omega}_j = \epsilon(t), \tag{4}$$

where $\epsilon(t)$ is defined as white noise with zero mean and unit variance. When comparing the heave motion estimation with the true state, which will be discussed later, it was shown that 4 could be solved independent of the remaining states without loosing any performance. By first solving (4) for each mode j, the remaining, uncoupled term of (3) can be presented as a linear system. Define the vector: $\mathbf{x}_j = [z_j,\ \dot{z}_j]^T = [x_{1,j},\ x_{2,j}]^T$. Each mode denote an oscillator and can be written in state space form:

$$\begin{aligned} \dot{\mathbf{x}}_j &= [x_{2,j},\ -\omega_j^2 x_{1,j}],^T \quad t > t_0,\ \mathbf{x}_j(t_0) = \mathbf{x}_{j,0}, \\ y_j &= -\omega_j^2 x_{1,j}, \end{aligned} \tag{5}$$

where $j = 1, 2, ..., N_m$. Each of the N_m modes are now modeled. Before we can implement the observer, one must compensate for certain errors when measuring heave acceleration:

$$a_{z,imu} = \sum_{j=1}^{Nm} y_j - cos(\theta)\, cos(\phi) g + b_z + \xi_z \tag{6}$$

where g denote gravity and is assumed constant, θ, ϕ respectively denotes roll and pitch angles, b_z and ξ_z denote sensor offset (or bias) and some noise. Eq. (6) illustrates that the measured acceleration signal will contain an offset. Therefore, denote an offset state: x_{off} that is modelled as a random walk parameter:

$$\dot{x}_{off} = \epsilon(t), \quad x_{off}(0) = -cos(\theta)\, cos(\phi) g, \tag{7}$$

To convert the system from continuous to discrete state space form, let $t_k = k\Delta t$, $k \forall \mathbb{N}$, where Δt is the sampling time of the observer. The initial state is calculated in the same way for the continuous and the discrete time system. The dynamics of the eigenfrequencies, ω_j, in (4) is solved first since it is decoupled from the rest of the system.

We obtain the complete state space system by adding all the N_m states of the modes together with the the offset state x_{off}, the entire system is solved for every time instance and re-initialized if a new mode is either detected or vanishes. The complete discrete system can be written in state space form:

$$\begin{aligned} \mathbf{x}_{k+1} &= \mathbf{A}\mathbf{x}_k \\ \mathbf{y}_k &= \mathbf{C}\mathbf{x}_k, \end{aligned} \tag{8}$$

where

$$\begin{aligned} \mathbf{x}_k &= [\ \mathbf{x}_{1,k},\ \mathbf{x}_{2,k},\ \ldots\ \mathbf{x}_{N_m,k}\ x_{off,k}]^T \\ \mathbf{C} &= [\omega_{1,k}^2,\ 0\ \omega_{2,k}^2,\ 0,\ \ldots\ \omega_{N_m,k}^2,\ 0,\ 1], \\ \mathbf{A} &= \begin{bmatrix} \mathbf{A}_1 & & & \{\mathbf{0}\} \\ & \mathbf{A}_2 & & \\ & & (\ldots) & \\ & & & \mathbf{A}_{Nm} \\ & \{\mathbf{0}\} & & 1 \end{bmatrix} \end{aligned} \tag{9}$$

where $\mathbf{A}_j = \begin{bmatrix} 1 & \Delta t \\ -\omega_{j,k}^2 \Delta t & 1 \end{bmatrix}$, $j = 1, 2, ..., N_m$, $\mathbf{x}_k$ is the $(2N_m+1\times 1)$ state space vector and $\mathbf{y}_k$ is the $1\times(2N_m+1)$ measurement vector and $\{\mathbf{0}\}$ covers the non-diagonal parts of $\mathbf{A}$ with zeroes.

The observer itself is implemented using a standard discrete time Kalman Filter. The process covariance matrix ($\mathbf{Q}$) is weighted in such a way that the modes with high eigenfrequencies are penalized compared to modes with lower ones. A suitable solution is to multiply each element in $\mathbf{Q}$, which is associated to a mode, with the corresponding eigenfrequency w_j . The covariance of the measurement noise equals the standard deviation of the sensor noise squared.

2.4 Step 4 - Transformation of Motion

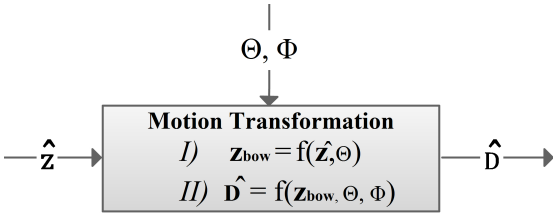

Fig. 5. Structure of the proposed heave motion transformation from $\{b\}$ to $\{p\}$

The output of the proposed observer is $\hat{\mathbf{z}}$ which is heave position and heave velocity at the location of the IMU. This section transfer the motion from this point to the bow tip, thus from the body fixed reference frame $\{b\}$ to the $\{p\}$ frame as illustrated in figure 1. We will divide the problem into two parts. In (I) we will translate the body fixed heave motion from $\{b\}$ to the bow tip. Let the axes point in the same body fixed directions. Denote this new coordinate frame as $\{b_{bow}\}$. Linear translation along the body fixed z axis of $\{b_{bow}\}$ is denoted $\mathbf{z}_{bow}$. In the second part, (II), we transform $\mathbf{z}_{bow}$ to the defined $\{p\}$ frame using Euler angle transformation.

Roll and pitch angles are required for the transformation. Since the angular output from an IMU is angular rate it is necessary to integrate these signals. Additional filtering is required in order to handle measurement errors such as drift and noise. It is assumed that the angular positions are correctly calculated and available for measurement using a method such as in Sabatelli et al. [2011]. Denote roll as ϕ and pitch as θ.

It is also assumed that the unwanted process disturbance, which will be discussed in section 3.1, will only have a very small impact on the calculation of roll and pitch angles. This assumption is made since the angular lab measurements shows no sign of the process disturbance frequencies. Thus, with correct handling of the angular rates, a smooth and accurate estimation of the angular positions will be made.

I) Transforming the motion from one point is discussed in chapter 7.5.4 in Fossen [2011] where one is assuming small roll and pitch angles. This results in a simplified linear transformation. Since the Wave Craft is a vessel designed to handle very rough seas, we will approach the problem without linearisation. The translation is illustrated in figure 6. Remember we are only interested in relative heave motion. It is assumed that both the IMU and the bow point is positioned at the centerline and share the same position on the baseline.

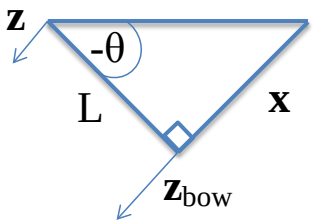

Fig. 6. Coordinate transformation from $\{b\}$ to $\{b_{body}\}$

where L is the longitudinal length from the location of the MRU to the bow tip. Note that the pitch is defined negative with the nose down according to the right hand rule. Hence:

$$\begin{aligned} \mathbf{z_{bow}} &= \hat{\mathbf{z}} + \mathbf{x} \\ &= \hat{\mathbf{z}} + L\,tan(-\theta) \\ &= \hat{\mathbf{z}} - L\,tan(\theta) \end{aligned} \tag{10}$$

II) To change coordinate system from the body fixed $\{b_{body}\}$ to the {p} frame we use section section 2.2.1 in Fossen [2011]. The results follow directly using the Euler angle transformation matrix:

$$\hat{\mathbf{D}} = cos(\theta)\,cos(\phi)\,\mathbf{z_{bow}} \tag{11}$$

3. RESULTS

As mentioned, the results in this section and figure 2 and 4 are based on time series from model test of a 3 meter long SES, namely the Wave Craft. The scale factor is 1 : 8. The peak detection is run online with $T = 15s$ (see section 2.2) The FFT has a certain memory sequence with $a_{z,imu}(k)$ as input in a first in, last out approach. The accelerometer used for the test is an [ICSensors, 2013] and the true heave position is read using [Qualisys, 2013]. Most axis are unified due to UM proprietary rights.

3.1 Severe process disturbances on the accelerometer

Figure 1 illustrates the lift fan that blows air into the air cushion. The cushion dynamics involves large large changes in net air flow due to nonlinear lift fan characteristics and sudden leakages under seals and through the ventilation valve. The dynamics will correspond in

accelerations denoted as process disturbances. Figure 7 illustrates the challenges that occur on a SES compared to other crafts when it comes to estimate heave motion using an accelerometer. The lift fan is turned off through the second half of the time series. When the fan is turned off, it is assumed that the process disturbances can be compared to craft such as catamarans or swaths. Figure 7 shows the time series of the air cushion pressure ($P_c(t)$), the accelerometer placed in the origin the $\{b\}$ frame ($a_{z,imu}$) and an accelerometer placed at the bow tip ($a_{z,bow}$).

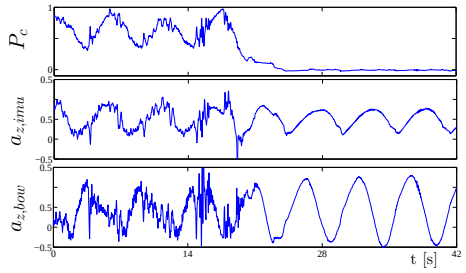

Fig. 7. The air cushion dynamics on a model test SES produce more process disturbances when the lift fans are on versus off. However, it is doubtful that the process noise is directly scalable for a full-sized SES. Regular wave, $T_p = 8.5s$

Note that the process disturbance is even larger on the bow tip. This is why we propose to transform the motion from the $\{b\}$ frame to the bow tip instead of estimating heave motion directly from the bow tip.

3.2 Heave Motion Estimator Performance

For the following results, the control system discussed in section 1.1 is at all times turned on. Two different time series will be shown using an irregular JONSWAP wave with $T_p = 8.5s$. First, we will illustrate heave motion estimation at the location of the MRU in the $\{b\}$ frame. On the following figure, this motion will be transferred to the $\{p\}$ frame where it will be compared to measurements of the true heave position. There will not be done any comparison between estimated heave velocity and the true heave velocity since these results are assumed better than of the position estimates (Küchler et al. [2011]). As previously, the output of the observer/estimator is denoted with a hat ($\hat{\diamond}$) and the true state without.

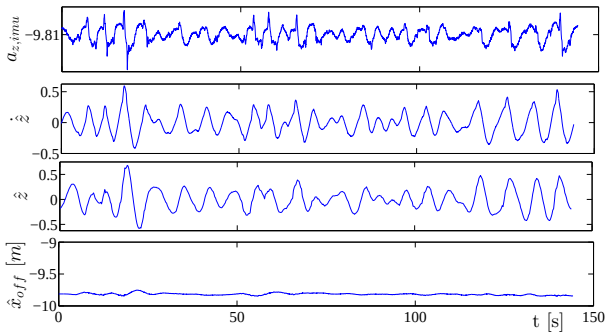

Fig. 8. The time series shows accelerometer signal and heave motion estimation in the $\{b\}$ frame.

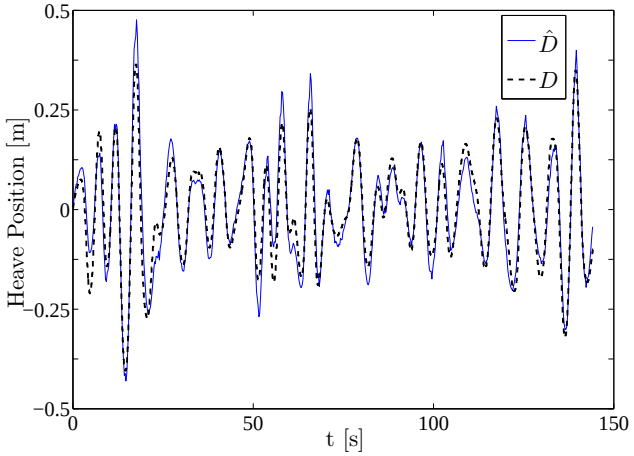

Fig. 9. The motion has been transformed from the $\{b\}$ frame to the $\{p\}$ frame where it is compared to the true heave position read by lab equipment.

Figures 8 and 9 illustrates the performance of the system with acceleration error terms such as gravity, measurement noise and process disturbance. The following figures, 10 and 11 illustrates the performance when we add an instant, fake, bias to the accelerometer, $b_{z,k} = 2$ at $t = \Delta t$. In other words, for each time step after the first, $a_{z,imu}(k) = a_{z,imu}(k) + b_{z,k}$. This illustrates the robustness of the system if a sudden bias or drift error appear on the signal.

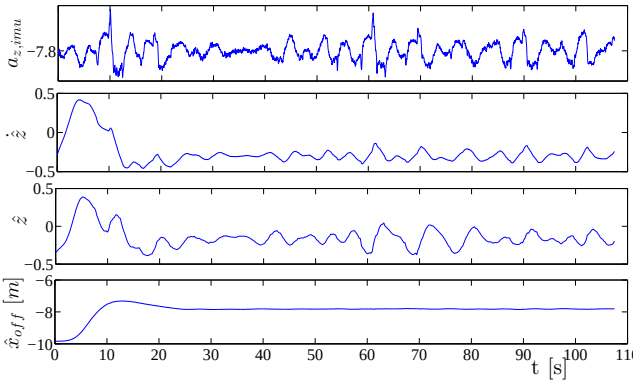

Fig. 10. Bias is added to the accelerometer, $b_{z,k} = +2$.

In figure 10, observe that the offset state converge to the correct value. The estimated heave motion also converges and does not experience any offset. All the figures illustrates that the process disturbances are rejected well since we do not want to expose the actuator to such oscillations in terms of wear and tear.

3.3 Estimate heave motion directly from an accelerometer located at the bow tip

In this section we will investigate the results if we place an accelerometer at the bow tip and use the proposed observer without any transformation of motion from the IMU to the bow tip as explained in section 2.4.1. Note that we are still transforming the motion to the $\{p\}$ reference frame as explained in section 2.4.2 in order to compare it to the true heave position. Figure 12 illustrate this scenario where

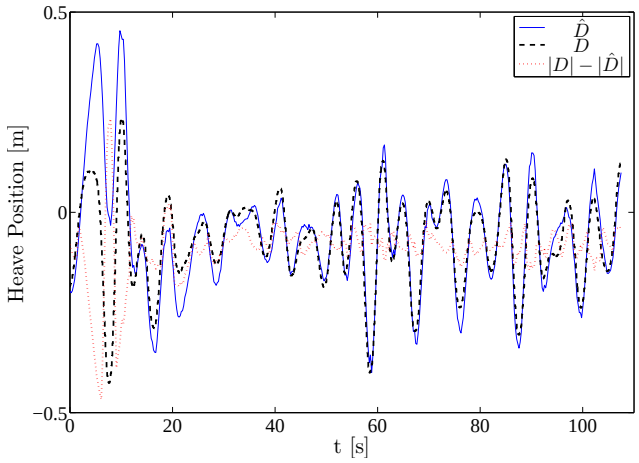

Fig. 11. Bias is added to the accelerometer, $b_{z,k} = +2$.

we denote $\hat{D}_{DIRECT}$ as the direct heave estimation. The time series used are the same as in figure 8. Therefore we will compare if it is best to position the accelerometer amidships and perform a transformation of motion to the bow, or just position the accelerometer directly on the bow tip. The observer remains unchanged in both cases.

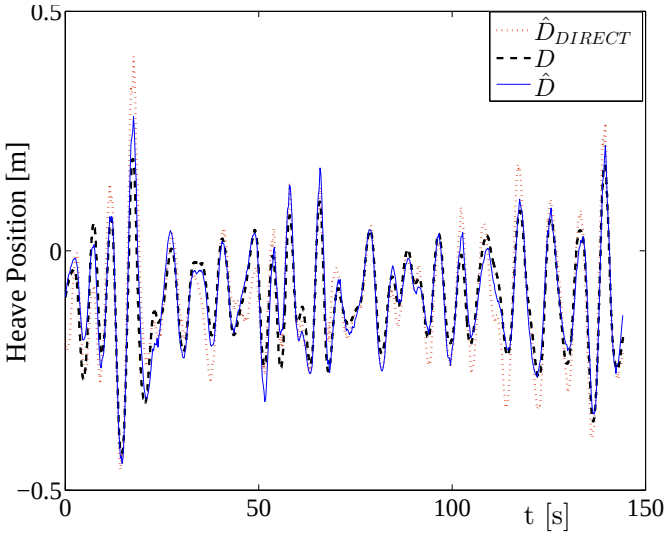

Fig. 12. Heave position estimation of an accelerometer placed at the vessel bow tip ($\hat{D}_{DIRECT}$) versus amidships ($\hat{D}$).

As expected, due to a larger process disturbance on an accelerometer placed on the bow tip, the performance is decreased using the direct approach.

4. CONCLUSIONS AND FURTHER WORK

We are interested in estimating heave motion at a specific point on a vessel in environments with high process disturbance. The case studied is a SES and we want to estimate heave motion at the bow tip. The focus is proper handling of an accelerometer signal, which includes unwanted terms for the heave motion estimation. Remember, the vent valve actuator are going to act accordingly to our estimated signals.

By studying the time series of the two accelerometers, one located at the bow tip and the other at amidships. We have seen that the process disturbance is larger at the former. Our results indicate that it is better to measure the acceleration at amidships, perform heave motion estimation and then transform the motion to the bow tip (D) in order to gain the highest performance.

According to figures 9 and 11, the heave motion estimation works as expected. However, the estimator fails to follow the true state at some points. These points are located at extreme heave positions. In this situation the actuator, that is assumed to act proportionally to the estimated heave motions, might saturate. This leads to a lack of compensation and can justify some of the deviation.

All in all the results are satisfactory and the estimation is usable as input signal for the controller.

Further work involves a study on how the process disturbances affects roll and pitch rates read by the IMU gyroscopes.

REFERENCES

Ø. Auestad, J.T. Gravdahl, A. J. Sørensen, and T. H. Espeland. Simulator and control system design for a free floating surface effect ship at zero vessel speed. *The 2013 IFAC Intelligent Autonomous Vehicles Symposium, Gold Coast (Australia), June 26 - June 28*, 2013.

S. Chakrabarti. *Handbook of Offshore Engineering*. Elsevier, Amsterdam, 2nd edition, 2008.

O. Faltinsen. *Sea Loads on Ships and Offshore Structures*. Cambridge University Press, Cambridge MA, 1993.

T. I. Fossen. *Handbook of Marine Craft Hydrodynamics and Motion Control*. John Wiley & Sons, Ltd, UK, 2011.

T. I. Fossen and T. Perez. Kalman filtering for positioning and heading control of ships and offshore rigs. *IEEE Control Systems Magazine*, 29 (6):32–46, 2009.

J.M. Godhavn. Adaptive tuning of heave filter in motion sensor. *OCEANS Conference Proceedings, Nice (France), September 28 - October 1*, 1:174–178, 1998.

ICSensors. Pressure sensors, accelerometers, and custom microstructures, model 3041. *http : //nees.berkeley.edu/Facilities/pdf/Instrumentation/ic_sensors_catalog.pdf*, 2013.

Kongsberg. Motion reference unit - mru. `http://www.km.kongsberg.com`, May 15 2013.

S. Küchler, J. Eberharter, K. Langer, K. Schneider, and O. Sawodny. Heave motion estimation of a vessel using accelerometer measurements. *18th IFAC World Congress, Milano (Italy), August 28 - September 2*, pages 14742–14747, 2011.

Qualisys. Oqus camera series. *http : //www.qualisys.com/products/hardware/oqus*, 2013.

S. Sabatelli, F. Sechi, L. Fanucci, and A. Rocchi. A sensor fusion algorithm for an integrated angular position estimation with inertial measurement units. *Design, Automation and Test in Europe Conference & Exhibition (DATE), Grenoble (France)*, 2011.